Int. J. Electrochem. Sci., 16 **(2021)** Article ID: 210530, doi: 10.20964/2021.05.42

International Journal of
ELECTROCHEMICAL
SCIENCE
www.electrochemsci.org

Mini Review

Metal-organic Framework (MOF) Based Materials for Electrochemical Hydrogen Production: A Mini Review

Xue Wang[*] *and Meng Sun*[*]

College of Electrical Engineering, Jilin Engineering Normal University, No.3050 Kaixuan Road, Changchun City, Jilin Province, 130052, P.R. China
[*]E-mail: xuewang@sutcm.net mengsun@vtcuni.com

Received: 1 January 2021 / *Accepted:* 3 March 2021 / *Published:* 31 March 2021

This paper reviews the research progress of some typical metal organic frameworks (MOFs) and MOF composites in the field of electrocatalytic hydrogen production over recent years. We conclude that MOF materials have excellent performance in the field of electrocatalytic hydrogen production based on their structural type, as follows: (1) pure MOF electrocatalysts; (2) MOF-supported composite electrocatalysts; and (3) MOF-derived electrocatalysts. We discuss the relationship between the internal structural characteristics of the materials and their electrocatalytic properties. This paper summarizes the design and synthesis strategies of these materials. Finally, we briefly discuss the prospects of their future development and propose possible issues.

Keywords: Metal organic frameworks; Electrochemical hydrogen production; Composite; Internal structure; Electrocatalyst

1. INTRODUCTION

In the 1970s, hydrogen started to be regarded as a carrier of energy. Hydrogen molecules not only have a very high energy density but can also burn in engines or convert into electricity in fuel cells. The only by-product of its formation is water, and no other harmful substances are produced. Compared with hydrogen energy, carbon-containing fossil energy may produce carbon monoxide, carbon dioxide and other harmful substances after combustion, causing great harm to the environment [1–5]. Hydrogen is one of the most abundant elements in the crust, but it does not exist in the form of molecular hydrogen under most conditions. Therefore, we must develop efficient and sustainable hydrogen production technology. However, to date, most hydrogen is still obtained through the natural gas refining process. This process not only consumes fossil energy but also produces greenhouse gases [6–10]. Therefore, using renewable energy for photovoltaic power generation is a clean and sustainable method for electrocatalytic hydrogen production in aqueous solutions [11–13].

As shown in Figure 1, we use acidic conditions as an example to introduce the HER mechanism. On the surface of the electrode, the HER can be divided into the following steps: (1) A hydrogen ion undergoes the Volmer reaction or a discharge reaction. In this step, a hydrogen ion combines with an electron on the electrode surface to form a hydrogen atom. Under acidic conditions, H3O+ is used as a hydrogen source, while under alkaline conditions, the hydrogen source is a water molecule. (2) H_2 can be formed by two different pathways [14–23]. One of them is via the Heyrovsky reaction (ion + atom reaction). In this reaction, the electron is transferred to the hydrogen atom and combines with another hydrogen ion in the solution to form H_2. The other pathway is via the Tafel reaction. Hydrogen ions in solution combine with electrons to form new hydrogen atoms, and two hydrogen atoms combine to form H_2. When most Pt-based metal materials are used as HER catalysts, the catalytic process occurs via the Volmer-Tafel reaction [24–30].

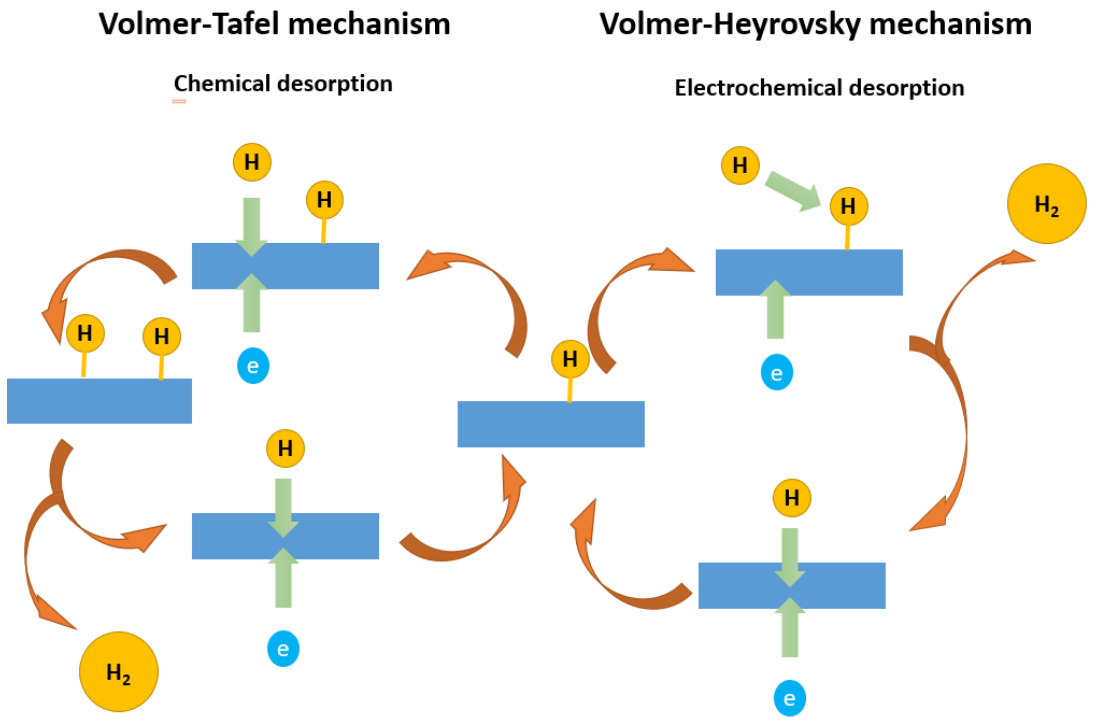

Figure 1. The reaction mechanism of HER on the electrode surface under acidic condition.

The Tafel slope is usually an important parameter to determine the HER mechanism. Based on the Butler-Volmer equation, the Tafel slope can be calculated. Its physical meaning is that the overpotential can affect the current value of an order of magnitude [31–38]. I) If the discharge reaction is very quick in the HER process, the binding reaction is a decisive step in the HER. The Tafel slope of this reaction is 2.3 RT/2F (29 mV/dec). II) If the HER rate is limited by the ion + atom reaction, the Tafel slope is 4.6 RT/2F (38 mV/dec). III) If the discharge reaction is very slow in the HER process, H_2 is produced by either a binding reaction or an ion + atom reaction. Its Tafel slope is 4.6 RT/F (116 mV/dec).

Electrocatalysts can accelerate the electrochemical reaction rate without being consumed. They can participate in electrochemical processes on the surface of the working electrodes or as the working electrodes. Electrocatalysts can assist electron transfer from electrodes to reactants or promote the transition of intermediate products in the electrocatalysis process [39–42]. Polarization is inevitable in the electrochemical process and results in a variety of impedance forms (resistance, capacitance, inductance). The starting potential of the electrocatalytic reaction exceeds the thermodynamic equilibrium potential, resulting in an overpotential [43–49]. Therefore, we need to find efficient catalysts to reduce the overpotential of electrocatalytic reactions. In recent years, perovskite oxides, noble metals and other related materials have attracted extensive attention, and the reaction mechanism of perovskite oxides as electrocatalysts has been well studied.

Metal organic frameworks (MOFs) are composed of porous crystals with three-dimensional, periodic and multidimensional network structures that are grown via the self-assembly of metal centres and metal clusters through coordination along with organic ligands [50–53]. In addition, MOFs have a highly developed pore structure. Previous studies have shown that MOFs have many potential applications, such as in gas storage, sensing, catalysis and supercapacitors.

MOFs are widely used in catalysis. In the field of electrocatalysis, MOF-based electrocatalysts can be used for hydrogen evolution, oxygen evolution, oxygen reduction and carbon dioxide reduction. MOFs have the characteristics of a uniform distribution of catalytic active sites and pores with a large specific surface area, and they can be loaded with other active substances. They can also form composites to enhance catalytic activity. This paper introduces the research progress of MOFs in the field of electrocatalytic hydrogen production via the HER.

2. PURE MOFs ELECTROCATALYST

In the design of pure MOF catalysts for the HER, the electrochemical catalytic activity of MOFs is the key factor. Qin et al. [54] reported superstable molybdate MOF electrocatalysts NENU-500 and NENU-501. Both MOFs are composed of Mo-based POM nodes ε-$PMo_8^{V}Mo_4^{VI}O_{36}(OH)_4Zn_4$ and ε-$PMo_8^{V}Mo_4^{VI}O_{37}(OH)_3Zn_4$ (Zn-ε-Keggin). Different organic connectors have been linked to MOFs. More specifically, the BTB compound $[TBA]_3[\varepsilon\text{-}PMo_8^{V}Mo_4^{VI}O_{36}(OH)_4Zn_4]$ $[BTB]_{4/3} \cdot$ xGuest (TBA = tetrabutylammonium) was used to link NENU-500. Mo and POM are two main components responsible for the electrocatalytic activity of the HER. The selection of Mo-based POM was also based on considering the tetrahedral arrangement of Zn cations used to construct 3D MOF structures. The results show that the combination of the advantages of POM and MOFs (extensible porous frameworks) can result in an excellent and stable HER performance. In 0.5 M H_2SO_4 electrolyte, the Tafel slope of NENU-500 is 96 mV/dec. Under a current density of 10 mA/cm^2, the overpotential is 237 mV. The Tafel slope of NENU-501 is 137 mV/dec [55–57]. Under a current density of 10 mA/cm^2, the overpotential is 392 mV. The catalytic performance of NENU-500 is close to that of commercial Pt/C. The results show that NENU-500 has superior performance to NENU-501 because of its open pore network, and the BET surface area is 195 m^2/g. NENU-501 is basically pore free because the TBA cation occupies the pore space. In addition, the performance of NENU-500 does not decrease significantly after 2000 cycles.

Dong et al. [58] reported a Co-MOF for HER applications. Co is composed of an MOF centre, while 2,3,6,7,10,11-triphenylene hexamercaptan (THT) and 2,3,6,7,10,11-triphenylene hexamine (THA) are connected. The interesting feature of these MOF catalysts is that HER active metal complexes CoS_2N_2, CoS_4 and CoN_4 are incorporated into a 2D framework via metal dithiolane coordination. The two-dimensional structure of the MOF can expose more active sites. In addition, the electrochemical stability can be enhanced by the successful immobilization of the metal complexes. In 0.5 M H_2SO_4 electrolyte solution, THAT-CO has a Tafel slope of 71 mV/dec. At a current density of 10 mA/cm^2, it shows an overpotential of 283 mV. At a current density of 10 mA/cm^2, the overpotential increases by 12 mV. When the current density reaches 10 mA/cm^2 after a reaction for 4 h, the overpotential increases by 34 mV, which indicates its stability in the HER.

Wu et al. [59] reported another representative pure MOF electrocatalytic HER material. CTGU-5 and CTGU-6 were synthesized based on polymorphic Co groups. Both MOFs are composed of a cobalt centre, naphthalene-1,4-dicarboxylic acid (L) and 1,4-bis (imidazolium) butane (BIB). The difference between the two MOFs is the coordination mode of the water molecule; H_2O is coordinated with the cobalt centre in CTGU-5, while it is linked to the skeleton of CTGU-6. The difference in the coordination mode can result in the hierarchical structure of both MOFs [60–62]. Electrocatalytic characterization of the HER in 0.5 M H_2SO_4 electrolyte showed that the overpotential and Tafel slope of both MOFs were 388 and 425 mV and 125 and 176 mV/dec, respectively. The satisfactory activity of CTGU-5 is due to its layered structure, which makes it easier for reactants to approach the active cobalt sites. The excellent activity of CTGU-5 was enhanced after adding acetylene black (AB). The results show that the composite (mixing ratio 1:4) has an overpotential of 44 mV at 10 mA/cm^2. The Tafel slope is 45 mV/dec. Under a 255 mV overpotential, the composite has 96-h stability in chronoamperometry.

Therefore, the key to the electrocatalytic activity of pure MOFs in the HER is the selection of metal nodes. However, the selection of organic linkers is another key point because they have a substantial effect on the final coordination structure and porous network, therefore affecting the electrocatalytic performance of the corresponding MOF catalysts. Table 1 shows the MOF electrocatalysts for the HER with the parameters.

Table 1. MOF electrocatalysts for the HER with the parameters.

Materials	Overpotential (mV)	Reference
[Metal–Carbon–(Benzene)$_i$–Chain]$_n$	-	[63]
AB&Cu-MOF	208	[64]
CTGU-9	98	[65]
Co-MOF	125	[66]

3. COMPOSITE ELECTROCATALYST LOADED ON MOFs

The advantages of using MOFs as substrates for other catalyst loadings are due to their high surface area and excellent pore volume. In addition, the synergistic effect between the MOF substrate

and the loaded catalyst may further enhance the electrocatalytic properties, which may also result in the occurrence of some interesting mechanisms. In addition to pure MOFs, the development of MOF-based composites has made great progress in recent years. By combining MOFs with conductive nanoparticles, MOF-based composites have the strengths of the two parent materials.

Hod et al. [67] reported the use of an MOF NU-1000 as a scaffold for the electrodeposition of Ni-S for the HER electrocatalysis. NU-1000 is a mesoporous MOF that consists of $Zr_6(\mu_3\text{-}O)_4(\mu_3\text{-}OH)_4(OH)_4(OH_2)_4$ as the metal node and TBA-Py^{4-}(1,3,6,8-tetra(p-benzoic acid) pyrene as the organic ligand. It can be grown on an FTO substrate as a rod structure. In addition, NU-1000 has a high resistance to hydrolysis with excellent chemical stability [68,69]. In 0.1 M HCl electrolyte, the prepared Ni-S film exhibited an overpotential of 238 mV with a Tafel slope of 120 mV/dec. At a current density of 10 mA/cm^2 for 2 h, it also showed good stability. The enhanced catalytic performance of the HER can be ascribed to the synergistic effect between Ni-S and water and the oxygen groups based on Zr_6 nodes. Short-range proton transfer and long-range proton transfer can be beneficial for local proton activity. Benzoic acid can be further used for modifying NU-1000. Compared with that of the original NU-1000-Ni-S, the electrocatalytic activity of benzoic acid-modified NU-1000 is obviously reduced.

Dai et al. [70] observed a similar phenomenon, and the work on UiO-66-NH_2 provides supporting information for the immobilization of molybdenum polysulfide (MoS_x). In the solvothermal synthesis of UiO-66-NH_2, $(NH_4)_2MoS_4$ was added simply to load MoS_x. The electrocatalyst exhibited an overpotential of 200 mV (10 mA/cm^2) with a Tafel slope of 59 mV/dec. In addition to the well-known advantages of the MOF catalyst, in this case, the MOF UiO-66-NH_2 based on Zr could modify the direct environment of sulfide-based catalysts to enhance HER catalytic activity. Table 2 shows the electrocatalyst-loaded MOFs for use in the HER with the parameters.

Table 2. Electrocatalyst-loaded MOFs for the HER with the parameters.

MOF	Loaded material	Overpotential (mV)	Reference
Co-MOF	CoP	49	[71]
N-MOF	W	53	[72]
MOF	Pd	85	[73]
NOTT-101	CuS	78	[74]

4. MOFs DERIVED ELECTROCATALYST

Transition metal sulfides and phosphates have strong electrocatalytic properties. In the preparation process, MOFs can be used as templates to generate electrocatalysts due to their unique pore structure. Compared with the application of pure MOFs and catalyst-loaded MOFs, more attention has been given to the production of large-scale metal-based catalysts using MOFs as precursors.

Wu et al. [75] reported a porous molybdenum carbide nano-octahedron synthesized from a Cu-based MOF (HKUST-1, $Cu_3(BTC)_2(H_2O)_3$, BTC = benzene-1,3,5-tricarboxylate). The guest

polyoxometalate unit is ($H_3PMo_{12}O_{40}$). This precursor is named NENU-5($[Cu_2(BTC)_{4/3}(H_2O)_2]6$-$[H_3PMo_{12}O_{40}]$). NENU-5 was annealed in a N_2 stream, resulting in the formation of MoC_x. In addition, Cu was embedded in MoC_x and then eliminated by $FeCl_3$, leaving a MoC_x nano octahedron for HER electrocatalysis. The electrocatalytic properties of MoC_x in the HER were investigated in H_2SO_4 and KOH. In 0.5 M H_2SO_4, a 142 mV overpotential was needed to achieve a current density of 10 mA/cm^2. In 1 M KOH, a 151 mV overpotential was needed to achieve a current density of 10 mA/cm^2. NENU-5 not only acted as a precursor but also limited the growth of MoC_x, resulting in uniform distribution and nanosized crystals. The amorphous carbon matrix provided additional protection for the embedded nanocrystals.

Yang et al. [76] synthesized a nitrogen-doped graphene layer coated with FeCo alloy nanoparticles derived from the bimetallic MOF precursor $Fe_3[CO(CN)_6]_2$. Since $Fe_3[CO(CN)_6]_2$ is rich in catalytic active metals and nitrogen, the formed FeCo alloy had a high content of N in the annealed products. In 0.5 M H_2SO_4, when the current density reached 10 mA/cm^2, the overpotential was 262 mV. The Tafel slope was 74 mV/dec. At a 300 mV over potential, it showed excellent stability after 10000 CV cycles and 10 h chronoamperometry tests. The good activity of the catalyst is due to the following characteristics: 1) compared with pure graphene, N doping can provide extra adsorption sites and reduce the free energy of adsorption (ΔGH); 2) introducing Fe atoms into the Co cluster (Co_4) can change the Co-Co bond length and introduce formed Fe-Co and Fe-Fe bond lengths, which can be customized to obtain an optimized ΔGH; 3) the metal and nitrogen can result in a synergistic effect to improve the performance of the materials; and 4) graphene shell-coated alloy NPs could prevent corrosion and enhance stability.

Raoof et al. [77] reported a (BTC)2 [BTC = 1,3,5-benzenetricarboxylate as porous template for preparation of a Cu/nanoporous carbon composite. The MOF-derived Cu/nanoporous carbon composite (Cu/NPC composite) is synthesized by direct carbonization of the MOF-199 without any carbon precursor additive. At the same time, the surface oxidation of MWCNTs to generate oxygen-containing groups and defect sites to dope the heteroatoms to achieve unexpectedly high OER catalytic activity was also firstly proposed. In addition, the composite of carbon nanotubes with other nanomaterials has also proven to be an important catalyst. The physical characterization of the solid catalyst is achieved by using a variety of different techniques, including XRD (X-ray powder diffraction), scanning electron microscopy, thermo-gravimetric analysis, and nitrogen physisorption measurements.

In addition to the synergistic effects and chemical composition, MOF-based precursors could have an impact on the structural transformation. Yu et al. [78] introduced the application of NiCo Prussian blue analogue (PBA) nanocubes ($Ni_3[CO(CN)_6]_2 \cdot 12H_2O$) as precursors for the production of NiS nanoframeworks. The preparation is based on the anion exchange between Ni-Co PBA and Na_2S. Because there are more defects at the edge than at the relatively smoother surface of the MOF, the exchange reaction was conducted first in these areas. The etching then moved from the edge to the less corrosive intermediate surface. The reaction induced by this structure led to the transformation of MOF nanocubes into NiS nanostructures. The obtained NiS nanostructures exhibited superior electrocatalytic properties in 1 M KOH. The overpotential was 94 mV at 10 mA/cm^2, and the Tafel slope was 139 mV/dec. The corresponding chronoamperometric test showed that the current only decreased by 8%

after 16 h of operation at 115 mV overvoltage. In addition to the catalytic activity of NiS for the HER, its excellent performance was related to the 3D framework structure.

In situ transformation of Mo-based MOFs into porous Mo_2C has been proven to produce highly active and stable β-Mo_2C/C heterostructures for the HER [79]. The two-step synthesis method involves impregnating the framework of MOFs (i.e., MIL-53 (AL)) with a Mo source and then carburizing the Mo_2C nanocrystals to nucleate and grow into a confined porous structure. The characterization results indicated the formation of mesoporous carbon with β-Mo_2C NPs (5-10 nm). The possible formation mechanism was proposed. The tendency of the catalyst to electrochemically catalyse the HER was tested in alkaline aqueous medium (1 M KOH). Compared with Pt/C and Mo_2C/XC72 black catalysts, the electrocatalyst showed significant HER activity at 10 mA/cm^2 and was stable for 20 h. The EIS results of Mo_2C/C are explained by quadratic constant, porosity and charge transfer. The HER follows the Volmer-Heyrovsky mechanism. Due to the unique metal carrier interaction, which may be due to the small particle size and good dispersion, Mo_2C/C exhibited excellent electrocatalytic activity for the HER in alkaline media. The Tafel slope of Mo_2C/C was 63.6 mV/dec, which is higher than that of Pt/C (55.7 mV/dec). However, it is lower than Mo_2C/XC72 (74.5 mV/dec). The electrocatalytic stability test of Mo_2C/C lasted for 20 h, and the overvoltage corresponding to the current density of 10 mA/cm^2 increased by 20 mV.

ZIF-67 is a cobalt-based MOF with 2-methylimidazole as the organic linker. It is one of the most commonly used MOF precursors for the HER. Yilmaz et al. [80] reported the preparation of NiCo-intercalated Co_9S_8 from ZIF-67. In a 1 M KOH electrolyte solution, the catalyst showed an overpotential of 142 mV and a small Tafel slope of 62 mV/dec at a current density of 10 mA/cm^2. The chronoamperometric test showed that there was no obvious current drop at a constant potential of 20 mA/cm^2 for 60 h, indicating its superior stability. Through the formation of a bimetallic isohydrogen sulfide hydroxide system and hollow structure, the conductivity and hydrogen adsorption on the catalyst were improved. Other reports indicated that N-doped carbon [81], Co@N-doped carbon nanotubes [82] and nickel phosphide [83] can be prepared as catalysts derived from ZIF-67.

Compared with pure MOFs and MOF-supported composite electrocatalysts, research suggests that MOF-derived electrocatalysts are more feasible. We can start with the MOF-derived electrocatalysts, adjust the structure of the catalyst for electrocatalytic performance, and increase the number of active sites to improve the electrocatalytic performance of the catalyst. Table 3 shows the electrocatalyst using MOFs as precursors for the HER with the parameters.

Table 3. Electrocatalyst using MOF as precursor for HER with the parameters.

MOF	Formed material	Overpotential (mV)	Reference
$Ni(bdc)_2(ted)$	Ni	88	[84]
ZIF-67-Co	CoP	86	[85]
MOF-199	Cu	200	[86]
ZIF-8	C	200	[87]
Co-MOF	Co-NC	84	[88]

Ni-MOF	A-Ni-C	34	[89]
Hofmann-type-based MOF	S-CoWP@(S, N)-C	35	[90]
MOF-74-Ni	Ni_2P/C	94	[91]
Ni-MOFs	NiSe@NC	123	[92]
Co-MOF	CoP-NS/C	59	[93]
CoNi-MOF	CoNiP	138	[94]
Co-MOF-800	Co–N-doped carbon	120	[95]
Mo-MOF	PtCu–MoO_2@C	42	[96]

5. CONCLUSIONS AND OUTLOOKS

In recent years, some MOFs and MOF-based composites have been successfully used as HER catalysts. Typical HER active sites in conventional catalysts, such as polyoxometalates, metal sulfides and metal nitrides, can be used to construct MOFs with acid resistance and HER activity. Similar to other properties of MOFs such as the coordination environment and accessibility of active sites, the porosity of the MOF structure and the size and morphology of MOF crystals are very important factors to determine HER performance. Although there are many studies on MOFs and their composites, the stability of MOFs and their composites still needs to be improved. Additionally, the mechanism of electrocatalytic hydrogen production needs to be further explored. Therefore, the exploration of MOFs and their composites in the field of electrocatalytic hydrogen production is still a common research focus.

ACKNOWLEDGEMENT
This work was funded by Doctoral project of Jilin Engineering Normal University (BSKJ201805)

References

1. H.-F. Wang, L. Chen, H. Pang, S. Kaskel, Q. Xu, *Chem. Soc. Rev.*, 49 (2020) 1414–1448.
2. H. Sun, Z. Yan, F. Liu, W. Xu, F. Cheng, J. Chen, *Adv. Mater.*, 32 (2020).
3. Q. Wang, K. Domen, *Chem. Rev.*, 120 (2020) 919–985.
4. Q. Wang, D. Astruc, *Chem. Rev.*, 120 (2020) 1438–1511.
5. M. Luo, Z. Zhao, Y. Zhang, Y. Sun, Y. Xing, F. Lv, Y. Yang, X. Zhang, S. Hwang, Y. Qin, J.-Y. Ma, F. Lin, D. Su, G. Lu, S. Guo, *NATURE*, 574 (2019) 81+.
6. R. Yang, Y. Zhou, Y. Xing, D. Li, D. Jiang, M. Chen, W. Shi, S. Yuan, *Appl. Catal. B-Environ.*, 253 (2019) 131–139.
7. C. Hu, L. Zhang, J. Gong, *ENERGY Environ. Sci.*, 12 (2019) 2620–2645.
8. S. Chandrasekaran, L. Yao, L. Deng, C. Bowen, Y. Zhang, S. Chen, Z. Lin, F. Peng, P. Zhang, *Chem. Soc. Rev.*, 48 (2019) 4178–4280.
9. A. Muthurasu, V. Maruthapandian, H.Y. Kim, *Appl. Catal. B-Environ.*, 248 (2019) 202–210.
10. L. He, J. Liu, Y. Liu, B. Cui, B. Hu, M. Wang, K. Tian, Y. Song, S. Wu, Z. Zhang, Z. Peng, M. Du, *Appl. Catal. B-Environ.*, 248 (2019) 366–379.
11. X. Wang, M. Sun, Q. Wang, *Ekoloji Derg.* (2019) 3235–3247.
12. M. Sun, X. Wang, X. Shang, X. Liu, M. Najafi, *J. Mol. Graph. Model.*, 92 (2019) 123–130.

13. Q. Wang, D. Shi, J. Zhang, X. Wang, Y. Si, C. Gao, J. Fang, S. Luo, *Chin. J. Chem. Phys.*, 32 (2019) 292.
14. Y. Yang, H. Yao, Z. Yu, S.M. Islam, H. He, M. Yuan, Y. Yue, K. Xu, W. Hao, G. Sun, H. Li, S. Ma, P. Zapol, M.G. Kanatzidis, *J. Am. Chem. Soc.*, 141 (2019) 10417–10430.
15. Y. Liu, S. Jiang, S. Li, L. Zhou, Z. Li, J. Li, M. Shao, *Appl. Catal. B-Environ.*, 247 (2019) 107–114.
16. Y. Jiao, Q. Huang, J. Wang, Z. He, Z. Li, *Appl. Catal. B-Environ.*, 247 (2019) 124–132.
17. Y. Li, Z. Yin, G. Ji, Z. Liang, Y. Xue, Y. Guo, J. Tian, X. Wang, H. Cui, *Appl. Catal. B-Environ.*, 246 (2019) 12–20.
18. L. Lin, Z. Yu, X. Wang, *Angew. Chem.-Int. Ed.*, 58 (2019) 6164–6175.
19. X. Yang, L. Tian, X. Zhao, H. Tang, Q. Liu, G. Li, *Appl. Catal. B-Environ.*, 244 (2019) 240–249.
20. Y. Wang, J. Zhao, Z. Chen, F. Zhang, W. Guo, H. Lin, F. Qu, *Appl. Catal. B-Environ.*, 244 (2019) 76–86.
21. I.S. Pieta, A. Rathi, P. Pieta, R. Nowakowski, M. Holdynski, M. Pisarek, A. Kaminska, M.B. Gawande, R. Zboril, *Appl. Catal. B-Environ.*, 244 (2019) 272–283.
22. X.-B. Meng, J.-L. Sheng, H.-L. Tang, X.-J. Sun, H. Dong, F.-M. Zhang, *Appl. Catal. B-Environ.*, 244 (2019) 340–346.
23. Y. Jiao, W. Hong, P. Li, L. Wang, G. Chen, *Appl. Catal. B-Environ.*, 244 (2019) 732–739.
24. Y. Guo, T. Park, J.W. Yi, J. Henzie, J. Kim, Z. Wang, B. Jiang, Y. Bando, Y. Sugahara, J. Tang, Y. Yamauchi, *Adv. Mater.*, 31 (2019).
25. H. Xu, S. Ci, Y. Ding, G. Wang, Z. Wen, *J. Mater. Chem. A*, 7 (2019) 8006–8029.
26. Z. Wang, C. Li, K. Domen, *Chem. Soc. Rev.*, 48 (2019) 2109–2125.
27. T. Ouyang, Y.-Q. Ye, C.-Y. Wu, K. Xiao, Z.-Q. Liu, *Angew. Chem.-Int. Ed.*, 58 (2019) 4923–4928.
28. S. Zhao, X. Lu, L. Wang, J. Gale, R. Amal, *Adv. Mater.*, 31 (2019).
29. L. Yang, J. Shui, L. Du, Y. Shao, J. Liu, L. Dai, Z. Hu, *Adv. Mater.*, 31 (2019).
30. X. Li, J. Yu, M. Jaroniec, X. Chen, *Chem. Rev.*, 119 (2019) 3962–4179.
31. J. Peng, X. Chen, W.-J. Ong, X. Zhao, N. Li, *CHEM*, 5 (2019) 18–50.
32. J. Pang, R.G. Mendes, A. Bachmatiuk, L. Zhao, H.Q. Ta, T. Gemming, H. Liu, Z. Liu, M.H. Rummeli, *Chem. Soc. Rev.*, 48 (2019) 72–133.
33. F. Lyu, Q. Wang, S.M. Choi, Y. Yin, *SMALL*, 15 (2019).
34. H. Jiang, J. Gu, X. Zheng, M. Liu, X. Qiu, L. Wang, W. Li, Z. Chen, X. Ji, J. Li, *ENERGY Environ. Sci.*, 12 (2019) 322–333.
35. W. Zhu, Z. Chen, Y. Pan, R. Dai, Y. Wu, Z. Zhuang, D. Wang, Q. Peng, C. Chen, Y. Li, *Adv. Mater.*, 31 (2019).
36. M. Zhang, Q. Shang, Y. Wan, Q. Cheng, G. Liao, Z. Pan, *Appl. Catal. B-Environ.*, 241 (2019) 149–158.
37. J. Xu, Y. Qi, C. Wang, L. Wang, *Appl. Catal. B-Environ.*, 241 (2019) 178–186.
38. C. Wei, R.R. Rao, J. Peng, B. Huang, I.E.L. Stephens, M. Risch, Z.J. Xu, Y. Shao-Horn, *Adv. Mater.*, 31 (2019).
39. H. Karimi-Maleh, M. Alizadeh, Y. Orooji, F. Karimi, M. Baghayeri, J. Rouhi, S. Tajik, H. Beitollahi, S. Agarwal, V.K. Gupta, S. Rajendran, S. Rostamnia, L. Fu, F. Saberi-Movahed, S. Malekmohammadi, *Ind. Eng. Chem. Res.*, 60 (2021) 816–823.
40. H. Karimi-Maleh, A. Ayati, R. Davoodi, B. Tanhaei, F. Karimi, S. Malekmohammadi, Y. Orooji, L. Fu, M. Sillanpää, *J. Clean. Prod.*, 291 (2021) 125880.
41. L. Fu, M. Wu, Y. Zheng, P. Zhang, C. Ye, H. Zhang, K. Wang, W. Su, F. Chen, J. Yu, A. Yu, W. Cai, C.-T. Lin, *Sens. Actuators B Chem.*, 298 (2019) 126836.
42. L. Fu, Y. Zheng, P. Zhang, H. Zhang, Y. Xu, J. Zhou, H. Zhang, H. Karimi-Maleh, G. Lai, S. Zhao, W. Su, J. Yu, C.-T. Lin, *Biosens. Bioelectron.*, 159 (2020) 112212.

43. Q. Liang, H. Jin, Z. Wang, Y. Xiong, S. Yuan, X. Zeng, D. He, S. Mu, *NANO ENERGY*, 57 (2019) 746–752.
44. T. Sun, L. Xu, D. Wang, Y. Li, *NANO Res.*, 12 (2019) 2067–2080.
45. J. Lai, B. Huang, Y. Chao, X. Chen, S. Guo, *Adv. Mater.*, 31 (2019).
46. K. Jing, W. Ma, Y. Ren, J. Xiong, B. Guo, Y. Song, S. Liang, L. Wu, *Appl. Catal. B-Environ.*, 243 (2019) 10–18.
47. J. Jiao, R. Lin, S. Liu, W.-C. Cheong, C. Zhang, Z. Chen, Y. Pan, J. Tang, K. Wu, S.-F. Hung, H.M. Chen, L. Zheng, Q. Lu, X. Yang, B. Xu, H. Xiao, J. Li, D. Wang, Q. Peng, C. Chen, Y. Li, *Nat. Chem.*, 11 (2019) 222–228.
48. T. Hisatomi, K. Domen, *Nat. Catal.*, 2 (2019) 387–399.
49. [Anonymous], *Int. J. Artif. ORGANS*, 42 (2019) 386–474.
50. L. Fu, Y. Zheng, P. Zhang, H. Zhang, M. Wu, H. Zhang, A. Wang, W. Su, F. Chen, J. Yu, W. Cai, C.-T. Lin, *Bioelectrochemistry*, 129 (2019) 199–205.
51. Y. Xu, Y. Lu, P. Zhang, Y. Wang, Y. Zheng, L. Fu, H. Zhang, C.-T. Lin, A. Yu, *Bioelectrochemistry*, 133 (2020) 107455.
52. H. Karimi-Maleh, F. Karimi, S. Malekmohammadi, N. Zakariae, R. Esmaeili, S. Rostamnia, M.L. Yola, N. Atar, S. Movaghgharnezhad, S. Rajendran, A. Razmjou, Y. Orooji, S. Agarwal, V.K. Gupta, *J. Mol. Liq.*, 310 (2020) 113185.
53. H. Karimi-Maleh, B.G. Kumar, S. Rajendran, J. Qin, S. Vadivel, D. Durgalakshmi, F. Gracia, M. Soto-Moscoso, Y. Orooji, F. Karimi, *J. Mol. Liq.*, 314 (2020) 113588.
54. J.-S. Qin, D.-Y. Du, W. Guan, X.-J. Bo, Y.-F. Li, L.-P. Guo, Z.-M. Su, Y.-Y. Wang, Y.-Q. Lan, H.-C. Zhou, *J. Am. Chem. Soc.*, 137 (2015) 7169–7177.
55. H. Karimi-Maleh, Y. Orooji, A. Ayati, S. Qanbari, B. Tanhaei, F. Karimi, M. Alizadeh, J. Rouhi, L. Fu, M. Sillanpää, *J. Mol. Liq.* (2020) 115062.
56. L. Fu, Y. Zheng, P. Zhang, H. Zhang, W. Zhuang, H. Zhang, A. Wang, W. Su, J. Yu, C.-T. Lin, *Biosens. Bioelectron.*, 120 (2018) 102–107.
57. H. Karimi-Maleh, F. Karimi, M. Alizadeh, A.L. Sanati, *Chem. Rec.*, 20 (2020) 682–692.
58. R. Dong, Z. Zheng, D.C. Tranca, J. Zhang, N. Chandrasekhar, S. Liu, X. Zhuang, G. Seifert, X. Feng, *Chem. Eur. J.*, 23 (2017) 2255–2260.
59. Y. Wu, W. Zhou, J. Zhao, W. Dong, Y. Lan, D. Li, C. Sun, X. Bu, *Angew. Chem.*, 129 (2017) 13181–13185.
60. J. Zhou, Y. Zheng, J. Zhang, H. Karimi-Maleh, Y. Xu, Q. Zhou, L. Fu, W. Wu, *Anal. Lett.*, 53 (2020) 2517–2528.
61. M. Zhang, B. Pan, Y. Wang, X. Du, L. Fu, Y. Zheng, F. Chen, W. Wu, Q. Zhou, S. Ding, *ChemistrySelect*, 5 (2020) 5035–5040.
62. L. Fu, Q. Wang, M. Zhang, Y. Zheng, M. Wu, Z. Lan, J. Pu, H. Zhang, F. Chen, W. Su, *Front. Chem.*, 8 (2020) 92.
63. T. Liao, L. Kou, A. Du, Y. Gu, Z. Sun, *J. Am. Chem. Soc.*, 140 (2018) 9159–9166.
64. X. Wang, W. Zhou, Y.-P. Wu, J.-W. Tian, X.-K. Wang, D.-D. Huang, J. Zhao, D.-S. Li, *J. Alloys Compd.*, 753 (2018) 228–233.
65. W. Zhou, Y.-P. Wu, X. Wang, J.-W. Tian, D.-D. Huang, J. Zhao, Y.-Q. Lan, D.-S. Li, *CrystEngComm*, 20 (2018) 4804–4809.
66. J.-W. Tian, M.-X. Fu, D.-D. Huang, X.-K. Wang, Y.-P. Wu, J.Y. Lu, D.-S. Li, *Inorg. Chem. Commun.*, 95 (2018) 73–77.
67. I. Hod, P. Deria, W. Bury, J.E. Mondloch, C.-W. Kung, M. So, M.D. Sampson, A.W. Peters, C.P. Kubiak, O.K. Farha, *Nat. Commun.*, 6 (2015) 1–9.
68. J.E. Mondloch, M.J. Katz, N. Planas, D. Semrouni, L. Gagliardi, J.T. Hupp, O.K. Farha, *Chem. Commun.*, 50 (2014) 8944–8946.
69. H. Wu, T. Yildirim, W. Zhou, *J. Phys. Chem. Lett.*, 4 (2013) 925–930.

70. X. Dai, M. Liu, Z. Li, A. Jin, Y. Ma, X. Huang, H. Sun, H. Wang, X. Zhang, *J. Phys. Chem. C*, 120 (2016) 12539–12548.
71. T. Liu, P. Li, N. Yao, G. Cheng, S. Chen, W. Luo, Y. Yin, *Angew. Chem.*, 131 (2019) 4727–4732.
72. W. Chen, J. Pei, C.-T. He, J. Wan, H. Ren, Y. Wang, J. Dong, K. Wu, W.-C. Cheong, J. Mao, X. Zheng, W. Yan, Z. Zhuang, C. Chen, Q. Peng, D. Wang, Y. Li, *Adv. Mater.*, 30 (2018) 1800396.
73. M. Nie, H. Sun, D. Lei, S. Kang, J. Liao, P. Guo, Z. Xue, F. Xue, *Mater. Chem. Phys.*, 254 (2020) 123481.
74. X.-Q. Wu, D.-D. Huang, Y.-P. Wu, J. Zhao, X. Liu, W.-W. Dong, S. Li, D.-S. Li, J.-R. Li, *ACS Appl. Energy Mater.*, 2 (2019) 5698–5706.
75. H.B. Wu, B.Y. Xia, L. Yu, X.-Y. Yu, X.W.D. Lou, *Nat. Commun.*, 6 (2015) 1–8.
76. Y. Yang, Z. Lun, G. Xia, F. Zheng, M. He, Q. Chen, *Energy Environ. Sci.*, 8 (2015) 3563–3571.
77. J.-B. Raoof, S.R. Hosseini, R. Ojani, S. Mandegarzad, *Energy*, 90 (2015) 1075–1081.
78. X. Yu, L. Yu, H.B. Wu, X.W. Lou, *Angew. Chem.*, 127 (2015) 5421–5425.
79. M. Qamar, A. Adam, B. Merzougui, A. Helal, O. Abdulhamid, M. Siddiqui, *J. Mater. Chem. A*, 4 (2016) 16225–16232.
80. G. Yilmaz, K.M. Yam, C. Zhang, H.J. Fan, G.W. Ho, *Adv. Mater.*, 29 (2017) 1606814.
81. J. Lin, J. He, F. Qi, B. Zheng, X. Wang, B. Yu, K. Zhou, W. Zhang, Y. Li, Y. Chen, *Electrochimica Acta*, 247 (2017) 258–264.
82. J.-S. Li, B. Du, Z.-H. Lu, Q.-T. Meng, J.-Q. Sha, *New J. Chem.*, 41 (2017) 10966–10971.
83. T. Tian, L. Ai, J. Jiang, *RSC Adv.*, 5 (2015) 10290–10295.
84. T. Wang, Q. Zhou, X. Wang, J. Zheng, X. Li, *J. Mater. Chem. A*, 3 (2015) 16435–16439.
85. L. Li, X. Li, L. Ai, J. Jiang, *RSC Adv.*, 5 (2015) 90265–90271.
86. J.-B. Raoof, S.R. Hosseini, R. Ojani, S. Mandegarzad, *Energy*, 90 (2015) 1075–1081.
87. J. Feng, H. Zhou, J. Wang, T. Bian, J. Shao, A. Yuan, *Int. J. Hydrog. Energy*, 43 (2018) 20538–20545.
88. X. Wang, J. He, B. Yu, B. Sun, D. Yang, X. Zhang, Q. Zhang, W. Zhang, L. Gu, Y. Chen, *Appl. Catal. B Environ.*, 258 (2019) 117996.
89. L. Fan, P.F. Liu, X. Yan, L. Gu, Z.Z. Yang, H.G. Yang, S. Qiu, X. Yao, *Nat. Commun.*, 7 (2016) 10667.
90. B. Weng, C.R. Grice, W. Meng, L. Guan, F. Xu, Y. Yu, C. Wang, D. Zhao, Y. Yan, *ACS Energy Lett.*, 3 (2018) 1434–1442.
91. S. He, S. He, X. Bo, Q. Wang, F. Zhan, Q. Wang, C. Zhao, *Mater. Lett.*, 231 (2018) 94–97.
92. Z. Huang, J. Liu, Z. Xiao, H. Fu, W. Fan, B. Xu, B. Dong, D. Liu, F. Dai, D. Sun, *Nanoscale*, 10 (2018) 22758–22765.
93. H. Li, F. Ke, J. Zhu, *Nanomaterials*, 8 (2018).
94. Y. Lu, Y. Deng, S. Lu, Y. Liu, J. Lang, X. Cao, H. Gu, *Nanoscale*, 11 (2019) 21259–21265.
95. Z. Pan, N. Pan, L. Chen, J. He, M. Zhang, *Int. J. Hydrog. Energy*, 44 (2019) 30075–30083.
96. C. Zhang, P. Wang, W. Li, Z. Zhang, J. Zhu, Z. Pu, Y. Zhao, S. Mu, *J. Mater. Chem. A*, 8 (2020) 19348–19356.